Optical Filters to Exclude Non-Doppler-Shifted Light in Fast Velocimetry

D. Goosman, F. Avara, J. Wade, A. Rivera

June, 19, 2002

U.S. Department of Energy

Lawrence
Livermore
National
Laboratory

Optical filters to exclude non-Doppler-shifted light in fast velocimetry

David Goosman, George Avara, James Wade and Anthony Rivera

The authors are with Lawrence Livermore National Laboratory
P.O. Box 808, L-281, Livermore, CA 94550
925-422-1630, fax 925-422-2382

ABSTRACT

We have used optical velocimetry for 25 years at LLNL to measure velocity-time histories of many dynamic experiments. In certain ones, the shifted light was often quite weak compared to non-shifted light returning from surfaces and imperfections in glass components. In an intensity-measuring VISAR system, this would mean failure, and even with Fabry-Perot (FP) based systems which handle multiple frequencies, data is lost where the fringes coincide.

We designed, constructed and successfully used an experimental facility for doing experiments under such conditions by selectively eliminating most of the non-shifted light. Instead of making experimental records which were mostly non-shifted light prior to the use of the filter, we now obtain records where almost all of the light is shifted. The first system had a maximum efficiency of 25% for the desired light, but another version is under construction with a maximum efficiency of over 50%. The first version excluded the non-shifted light by a factor of 300 when manually tuned, and by 150 when run in a Window-based auto-tuning mode.

Our first version used a 50 mm diameter FP as the filter with a spacing of 1.65 mm and reflectivities of 77%. It was constructed for use in one of our 5-beam velocimeters. Rather than using five separate filters, we multiplexed all five records so that the desired light would reflect from the filter FPI and image onto separate fibers. These five output fibers then fed our standard tau-table with 5 cameras as described in our report for the 1996 HSPC in Santa Fe, USA.

One use of the filter system involved embedding optical fibers in long sections of explosives to make continuous detonation velocity-time histories. To date we have recently carried out 6 tests with this new facility, and two prior ones without. Explosive safety required that four shutters be used to assure that no significant light could illuminate the explosive from the end of the embedded fiber when personnel were close. An arrangement allowing the same system to use one filter FPI for 10 optical fibers can be made.

An astrophysical test suggested by J. Osher of LLNL on the origin of stellar redshifts was carried out with another version of this filter. The light was reflected four times from the same FPI to provide a efficiency of about 40% for the desired light and a rejection of the non-shifted light by a factor measured at more than 4 million to one, with a rejection bandpass of a few GHz.

Keywords: velocimetry, filters

1. INTRODUCTION

Optical velocimetry is used at LLNL to measure the time dependent velocity of surfaces accelerated by gas guns, exploding foils and explosives[1]. We have used both VISAR and Fabry-Perot interferometer systems for this purpose. Since the Fabry systems can handle more than one frequency of return light, our group has used those systems exclusively for the last 17 years. Our manybeam velocimeter system was described briefly at a recent Congress[2], at which time we had 10 of the 20 channels of recorders in use.

Several years ago, the first author was shown records taken at LANL by W. Hemsing[3] done to measure continuous detonation velocities within explosives. This was accomplished by monitoring the frequency of light reflected from the moving crushed fiber end within the explosive. Two such experiments were then carried out at LLNL in 1998. The data made sense, but was frequently obscured by non-Doppler shifted light that was an order of magnitude stronger than the data sought. We therefore devised a filtration system to mostly eliminate the non-shifted light to obtain better records.

Placing optical fibers within explosives to measure continuous detonation velocities can result in large amounts of undesired non-Doppler shifted light scattering from fiber imperfections and connections. We have designed and constructed a special filtration system, based upon angled fiber connections and a Fabry-Perot etalon that reduces this undesired light by a factor of more than 100, thus helping to make possible a whole new field of shock velocimetry inside materials.

2. EMBEDDED FIBER OPTICS

A typical embedded fiber experiment with a fiber being enveloped by a detonation wave is shown in fig. 1.
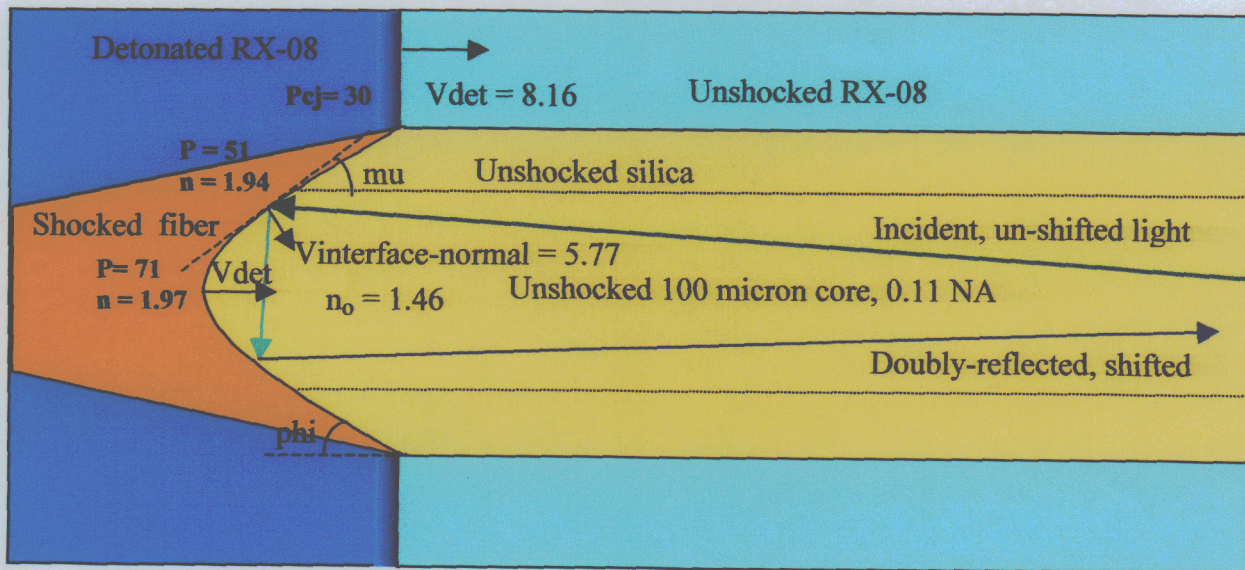
Figure 1. Approximate shape of the end of a crushed fiber embedded in RX-08HD explosive. Pressures are in GPa, as calculated by Souers[4], the refractive index is N, and velocities are in mm/usec.

It is a challenge for hydrodynamic codes to have the spatial resolution to model a 100-micron diameter optical fiber end, as well as to include enough of the explosive volume to make the problem meaningful. If the shock speed in the silica fiber core does not outrun the detonation velocity, V_{det}, a self-similar cup-shaped interface propages to the right at the speed = V_{det}. For this example, the index rises from 1.46 to about 1.9 at the interface.

The first author has calculated how much the reflectivity drops if the index change is not rapid with distance, by solving the wave equations for propagation through a material of varying index. If the interface transition region is thicker than about 20% of the wavelength in the unshocked material, then the reflection from this interface is less than half of that for a sharp interface. The uncertainty in the transition width is one of the two reasons why it is difficult to predict the amount of reflected light.

Figure 2. The calculated reflectivity of a boundary whose index rises linearly with distance from 1.46 to 1.9, as a function of the width of the transition region, measured in units of waves in the starting material.

The other reason is the uncertainty in the shape of the interface. If the center of this interface is nearly flat, then some light within the 0.11 NA can reflect once from this flatter portion and still be within the 0.11 NA of the fiber. This contribution is esti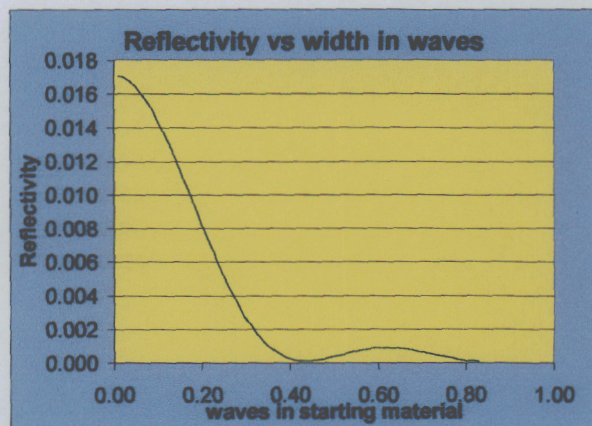mated to be about 1e-5 of the incident light. A more important contribution is the doubly reflected light, which samples an annular region of the interface. The area of this useful annulus is usually much larger than the area of the flat part mentioned earlier, but the two reflections mean much less intensity per unit area that from a single reflection. A Monte-Carlo program for Excel was written, and runs showed that for interfaces with a region that has a near 45 degree slope, most of the returned light is from two reflections. However, granulation of the interface, if it occurs, could further reduce the reflected light that is within 0.11 NA.

The frequency of light Doppler shifting from a solid surface, such as a diffuse metal, depends only upon the particle velocity, incident laser and collection direction vectors, and not upon the surface normal direction, as shown experimentally[5]. However, a shocked interface in a transparent material also has a Doppler-shifted reflection, which is known by normal-incidence experiments done at LLNL to be a direct measure of the shock speed, and not the particle velocity behind the shock front. But we care about the correct shift for light incident at an angle to the shock front. This situation is analgous to reflecting light from a moving, non-shocked rectangular plate of glass moving through air, where the normal to the plate is at an angle to the direction of the light. Thus the Doppler-shift from each reflection at the interface is given by the vector product

$$V_{apparent} = (\text{Index of unshocked silica})*V_{interface}*(K_{incident} - K_{reflected})/2) \tag{1}$$

Where bold fonts indicates vectors, and the K vectors are of unit magnitude and simply indicate direction. The index of refraction of the unshocked silica multiplies the normal velocity vector product, because the interface moving at V_{det} is overtaking wavecrests in the unshocked silica which are closer together than they are in air (by a factor of n = 1.46). $V_{interface} = V_{det}$ if the solution is self-similar as mentioned above.

Many hydrocalculations for self-similar solutions indicate that the particle velocity behind the shock in the silica is very nearly normal to the interface. In this case it is easy to show that

$$V_{interface-normal} = V_{det}*\sin(mu) , \tag{2}$$

where mu is the angle of the interface relative to the fiber axis.

Silica is usually characterized by means of single shock experiments to give the relation between shock speed and pressure, which we call the U_S-P curve. The crushed-fiber hydrocalculations provided by C. Soures[4] of LLNL, (which are not single shock experiments) indicate the the pressure at the axis on the interface is close to the value on U_S-P curve, if one sets $U_S = V_{det}$. For example, at the point shown on figure 1, 71 Gpa is close to the pressure on the silica U_S-P curve for a U_S value of 8.16 mm/usec. One

might speculate that as V_{det} is increased, the angle phi shown in figure 1 decreases to increase the pressure at the axis so that it matches that needed for U_s to match V_{det}. Further calculations will show if this is true.

In eqn. (1), $V_{apparent}$ varies from n_o*V_{det} to a smaller value depending upon the K directions. The Monte-Carlo program mentioned above also tallies the total Doppler shift from each interface reflection and gives a spectrum of shifts for the light that is reflected and transported back through the fiber to the velocimeter analysis table. For 0.11 NA fibers, the result is that the average shift due to the finite NA is quite small: the apparent velocity should be multiplied by 1.0014 to correct for the NA effect.

Doubling the NA of the fiber will increase the Doppler broadening of the reflected line by a factor of about 4 as well as collecting more light. But our Fabry system cannot use more light than that carried by a 100 micron 0.11 NA fiber anyway[2]. However, 0.22 NA fibers may in fact make more useful light than 0.11 fibers, and unless the shape of the interface is known, one needs to answer this question experimentally.

If the energy release upon detonation is spatially inhomogeneous, then the interface may have ripples or severe tilts rather than have the smooth symmetric shape shown in figure 1. We plan to use hydrocodes to model this, and to compare with data we have taken.

3. ANGLED CONNECTORS AND FIBER ENDS

Non-shifted light can arise from imperfections within the fiber, reflections from the fiber-air interfaces and scattering from dust on the optical elements. To greatly reduce the fiber-air interface reflections, we angled the entrance ends of the fibers carrying high laser power to the explosive. A nine-degree angle on the end of the fiber was sufficient to assure that reflected light missed the optical lens illuminating that fiber. The same angling was used for the one connector between the fiber embedded into the explosive and the fiber going to the filter. This scheme reduces the connector reflections from about 4% for normal connectors to about 100 times less. We do not use coupling fluid since the power level is high.

4. THE NON-SHIFTED LIGHT FILTRATION SYSTEM

To further reduce non-Doppler-shifted light, a filtration system based upon a closely-spaced Fabry Perot interferometer was designed. A Fabry interferometer can have its spacing set to transmit the non-shifted light and reflect almost everything else. Denoting the intensity reflectivities of mirrors 1 and 2 as R_1 and R_2, the intensity transmission as T_i, and the absorption coefficient of the mirror as A, then it is straightforward to show that for non-striped interferometers, the following relationships are valid:

$$T_i + R_i + A = 1 \quad (i = 1, 2) \text{ for each mirror.} \tag{3}$$

For light incident at an angle theta to the normal to the mirrors, the general expressions for the transmission and reflection of the interferometer, for identical mirrors and reflectivities above about 60%, are[6]

$$\text{Transmission} = T^2/((1-R)^2+4R\sin^2(phi/2)), \quad \text{and} \tag{4}$$

$$\text{Reflection} = R + T (TR-2R\cos(phi)+2R^2)/((1-R)^2+4R\sin^2(phi/2)), \tag{5}$$

where

$$phi = 4(pi)H(nu)\cos(theta)/c \tag{6}$$

is the phase change due a round-trip pass through the interferometer, and

$$R = R_1 = R_2 \tag{7}$$

is the reflectivity of each mirror. H is the mirror spacing, nu and c are the frequency and speed of the light and theta is the polar angle between the light and the surface normal to the FP mirrors.

Equations (4) and (5) apply for measurements taken in a plane where the multiple beamlets created within the interferometer are brought to superposition outside the interferometer, such as at the focal plane of a lens downstream of the interferometer. If the transverse walk of the many beamlets is small compared to the beam speckle diameter at the exit of the interferometer, then all the beamlets are in nearly perfect superposition even without the usual focussing lens. If not, then the relationships apply at the focal plane of a lens used to bring all of the beamlets into superposition.

It is apparent from eqn. (4) that one desires most of the beam to be close to normal incidence to the mirrors to achieve maximum transmission. In the system to be described below, which uses one FP filter for 5 velocimetry measurements, it is necessary to keep all of the fibers as close together as possible and to have the same polar angle with respect to the normal to the FP mirrors to minimize filtration inefficiencies due to angular spread. The maximum and minimum transmissions are

$$T_{max} = T^2/(1-R)^2, \quad \text{and} \tag{8}$$

$$T_{min} = T^2/(1+R)^2 \tag{9}$$

The most useful expressions are the reflected intensity when the transmission is peaked (achieved by adjusting the spacing or frequency, for example), which is

$$\text{Reflection (at Tmax)} = R+T(TR-2R+2R^2)/(1-R)^2, \tag{10}$$

and the reflected intensity when the transmission is near minimum, which is

$$\text{Reflection (at Tmin)} = R+T(TR+2R+2R^2)/(1+R)^2 \tag{11}$$

The idea is to use the reflected beam from the filter interferometer which will have a much reduced non-shifted component and send it to the usual velocimeter analyser table (with its own interferometer) for analysis. Table 1 illustrates numerical examples.

		A	0.00200	0.00200	0.00200	0.00200	0.00000
		R1	0.71000	0.77000	0.85000	0.90000	0.90000
		R2	0.71000	0.77000	0.85000	0.90000	0.90000
		T1	0.28800	0.22800	0.14800	0.09800	0.10000
		T2	0.28800	0.22800	0.14800	0.09800	0.10000
Unshifted	At peak transmission	Transm	0.98625	0.98268	0.97351	0.96040	1.00000
Unshifted	At peak transmission	Refl	0.00003	0.00006	0.00015	0.00036	0.00000
Shifted	At minimum transm	Refl	0.96930	0.98115	0.99144	0.99524	0.99723
Shifted	At minimum transm	Transm	0.02837	0.01659	0.00640	0.00266	0.00277

Table 1. Numerical examples of the transmission and reflection formulae.

This table shows shifted and non-shifted amounts for 4 combinations of mirror reflectivities ranging from 0.71 to 0.90, assuming perfectly flat mirrors. The last column shows that if the absorption A is zero, which is unrealistic, the reflectance at peak transmission falls to zero.

The critical row is the reflection of non-shifted light when the filter is set at peak transmission, which varies from 0.00003 to 0.00036. We want this value to be low so the experiment is not contaminated with too much non-shifted light. Reducing the mirror reflectivities from normal 0.9 values to 0.71 helps in two ways. First of all, the non-shifted reflectance gets 12 times smaller, and it becomes less sensitive to having exactly the correct mirror spacing, H. The slight penalty for this is that the reflectance of the shifted light, which we want to be large, drops from 0.995 to 0.969.

A plot of the reflectance and transmission of a filter with $R_1 = R_2 = 0.71$ is shown at the bottom of figure 3 as a function of frequency. The latter of which has been converted to the product of the interface velocity and the index of refraction, as detailed in eqn. (1).

Figure 3. The filtration system to reduce non-shifted light.

The graph in figure 3 assumes that the filter mirrors were first made parallel by using CW light into fiber # 7. Then the mirror spacing was set to minimize the non-shifted reflection for pulsed light injected into the fiber #6. This is because the exact wavelengths of the CW and pulsed laser are different and because the shot fibers and fiber #6 are off axis, whereas fiber #7 is on axis. Off-axis fibers have minimum reflection at mirror spacings about 0.005*waves larger than for on-axis fibers.

5. OPERATION OF THE FILTER SYSTEM

High power light from the laser beam farm is injected into 5 of the 7 fibers in fiber holder A, as shown in figure 3. We have repeatedly put 116 watts of 532 nm light for 50 microseconds into each one without damaging anything. This light is unpolarized by virtue of having traversed several meters of step-index 50-micron diameter and 0.11 numerical aperture multi-mode fiber. The light is collimated as well as can be done (limited by the fiber diameter) by a 100-mm focal length 25 mm diameter achromat lens. Half of this light passes through the lower polarizing beamsplitter cube shown in figure 3. The rest is wasted into a piece of black paper (but could be used by a more elaborate 10-fiber version of this system). The 50% that passes through the cube is imaged onto a similar 7 fiber chuck C, except the fiber diameter is now 100 microns instead of 50, to facilitate high power alignment. This way, there is much less chance of a poorly-aligned beam hitting the polyimide on chuck C and burning it. Fiber chuck C is angled to prevent reflection from its surface from entering the system. In addition, this angling aids a simple viewing system,

which uses a small CCD camera with a tiny mirror that is placed to intercept this reflected beam (but not much of the incident beam). This viewer allows us to see the 7 fiber cores and the 5 beam spots simultaneously to assure proper registration. The C fibers leading to the shot tank porthole are 15 m long. These ends are also angled, as are the matching ends of the 10-foot fibers that extend into the explosive.

Light from each fiber reflects from the moving interface in the explosive, is Doppler-shifted and returns along the same fiber to chuck C. The 50% of that light which is horizontally polarized is reflected by the lower cube to the upper one. There it is 100% reflected to a quarter-wave plate and into the filter. Here the spacing of the filter has been set to efficiently transmit the non-shifted light (from connector reflections, bubbles and imperfections in the fiber) and reflect efficiently the shifted light from the shock in the explosive. This shifted, reflected light passes through the quarter-wave plate a second time, giving it a vertical polarization allowing it to pass through the upper cube and be focussed onto the 7-fiber chuck B. That chuck is angled also. A CCD viewer takes advantage of this, allowing alignment of the chuck B using the light reflected from it.

The shifted light entering the fibers of chuck B goes to the usual manybeam velocimeter analyser table[2] to record the data. One unit of light fed to the analyser table on these 0.11 NA fibers is equivalent to about 2.5 units of light fed to the same table on the usual 0.22 NA fibers. This is because the standard nested lens probes used on most common velocimetry shots collect light into 0.22 NA fibers and the analyser table normally uses only the 0.11 NA part of that light. Presently the normal analyser table input is to a 1-meter long 0.22 NA 100 micron fiber. We have found that these short fibers, when injected with 0.11 NA light, emit at about 0.13 NA. We are building a 0.11 NA replacement fiber chuck for this 1 meter section.

6. TUNING THE FILTER

A considerable effort has gone into learning how to align and tune the filter system. One procedure is mentioned here. The filter mirrors are close to parallelism to start with.

The collimation of the beams from chuck A are determined by placing a 45 degree mirror just to the right of the lower cube. This reflects light to another head-on mirror placed about 40 cm away. A white card with aluminum foil on one side with two 1 mm holes placed about 7 mm apart is placed in the beam just downstream of the 45 degree mirror to verify that the two reflected spots have the same separation on the card as the holes have. If not, then the distance between chuck A and its lens is changed. The lower cube is on a tilt-rotation stage, and is adjusted so that reflections from its left face miss the fiber area of chuck A.

To adjust the position of the lens for chuck C, the CCD viewer is positioned so that it is focussed onto the fibers of chuck C. Then with low power light injected into the five outer fibers and the CCD viewer indicates whether the 50 micron images of these beams at chuck C are in focus (and registered). If not, the lens for chuck C is moved.

To retro-reflect the filter, we inject low power light into the center fiber of chuck C and place the paper-aluminum viewer card just to the left of the quarter wave plate. The filter is adjusted so that non-shifted light is reflected (as opposed to where it will be during a shot condition). The two tilt adjustments for the filter Fabry are moved until the reflected light falls on the hole in the card. The quarter wave plate is rotated until the beam heading toward chuck B is maximum.

The lens position for chuck B is adjusted by attaching short "stub" fibers to the ends of the chuck C fibers which are located in or near the shot tank. These stubs are angled on one end and not on the other. The angled end connects with the (angled) end of the long shot fibers. This allows about a 4% reflection to occur for aid in alignment. The stubs are removed prior to hooking up the shot, of course, to minimize reflections. Now low power light is injected into the 5 fibers of chuck A, and the weak reflection from the stubs passes through the entire system and images onto chuck B. Since the viewer for chuck B is already

focussed on the fiber ends, one verifies that the spots of light are also in focus, if not, then the lens for chuck B is moved. Registration of the spots with the fiber cores of chuck B is done at this time also.

7. FINE-TUNING THE FILTER AND MAXIMIZING THE EXTINCTION RATIO

We presently use the center fiber for making the filter mirror parallel by maximizing the extinction ratio, although that is not the only way to do it.

With only the CW beam on, we inject into the center fiber of chuck C. With low reflectivity mirrors, tuning on a reflected beam is more sensitive than using the usual method of tuning for parallelism with the transmitted beam. One of us, (GA), noticed in the transmitted pattern both the usual bright beam and a weaker beam below it that looked like the reflected beam. The latter is conjugate to the transmitted beam, when the one is bright, the conjugate beam is dark. We transported that weak image of the reflected beam into another CCD viewer so that it could be seen either from the filter room or the control room.

The extinction ratio is the ratio of reflected intensity at maximum vs. minimum as we adjust the common spacing between the filter mirrors. This ratio can be monitored from the control room by a camera viewing the power meter connected to fiber #7 of chuck B. When tuning locally, we obtained a ratio of 300. We found that if the filter is tuned initially locally, we could then vacate the room and go to the shot-control room and keep it in tune sufficiently so that we could obtain a ratio of 200. We used the tuning computer program written by one of us (GA), and using a very fine range on the piezo stack voltage driver.

The exact frequency of the pulsed laser is different than that of the CW laser that was used to assure the filter mirrors were parallel. Therefore, we need the pulsed beam to set the filter spacing to resonantly transmit the non-shifted pulsed light. Since personnel are not in the filter room during a shot, apparatus was built to monitor the amount of reflected pulsed light at the control room, and to adjust the spacing up to the last few seconds prior to the detonation of the shot. Light from the fiber#6 of chuck B is monitored on a photodiode viewed by an oscilloscope. The filter tuning computer operator in the control room changes the three piezo voltages and the common voltage every few seconds to keep the oscilloscope trace to a minimum height (lowest light level), assuring a proper filter spacing. This minimizes the non-shifted pulsed light that will be there and might obscure the desired shifted velocimetry record.

8. EXPERIMENTS WITH AND WITHOUT THE FILTER

Figure 4 is an early experimental result with a fiber in detasheet explosive, but prior to the construction of the filter. Although the detonation velocity lines are visible, they are heavily obscured by intense non-shifted light. Even the SBS lines (downshifted by 32.8 GHz due to high power) are equal in strength to the shifted lines.

Figure 5 shows the data taken with LX-17 explosive. The baseline non-shifted light at the beginning is mostly due to reflection from the explosive near the end of the embedded fiber. After the shock arrives, this source disappears, and the remaining non-shifted light (shown for about 300 nsec in figure 5) is intentionally produced light, since a small amount is useful for calibration. We first use the filter to make the non-shifted light negligible, and then inject downstream of the filter a small but controlled amount of non-shifted light from the laser.
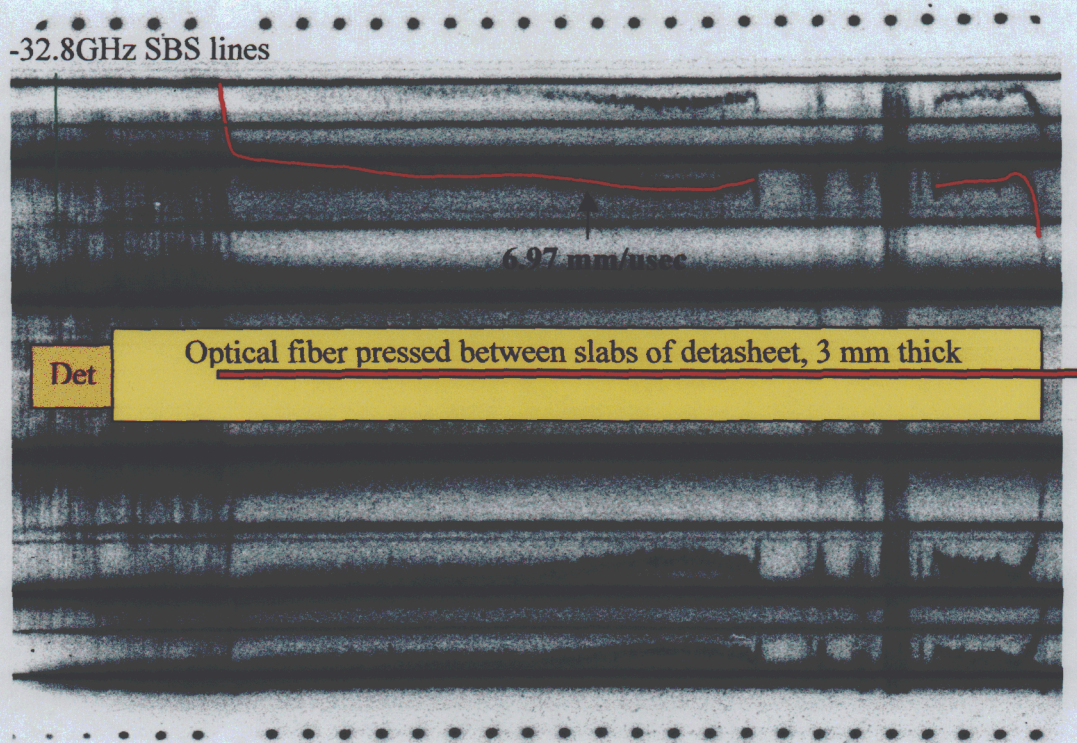
-32.8GHz SBS lines

6.97 mm/usec

Det — Optical fiber pressed between slabs of detasheet, 3 mm thick

Figure 4. A Fabry-Perot velocimetry record taken without the filter. Undesired non-shifted light dominates.

500 nsec time markers
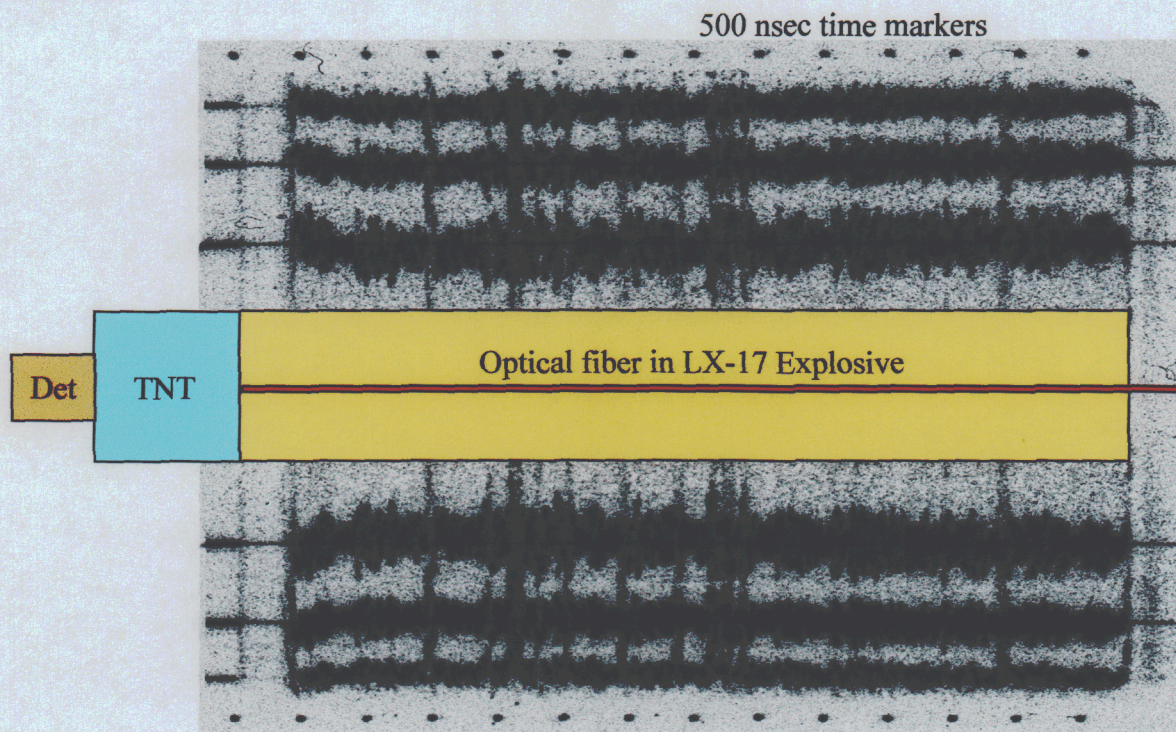
Det | TNT — Optical fiber in LX-17 Explosive

Figure 5. A record taken on LX-17 explosive with the filter. The detonation velocity just exceeds 12 orders of interference. Undesired non-shifted light has been eliminated.

A filter such as this could be used in conjuction with an intensity-measuring VISAR velocimeter to eliminate the non-shifted light, which can cause analysis errors if large enough and unforseen[7].

9. HIGH EXTINCTION RATIO FILTER

We designed and constructed a special filter for an astrophysical experiment suggested by J. Osher of LLNL. We were searching for an extremely weak frequency-shifted component in the presence of intense unshifted light.   The beam is resonantly reflected four times from the same Fabry filter. Measurements showed that the filter reflects 40% of the desired shifted light, and rejects unshifted light by a factor exceeding 4 million, with a bandpass of a few GHz.
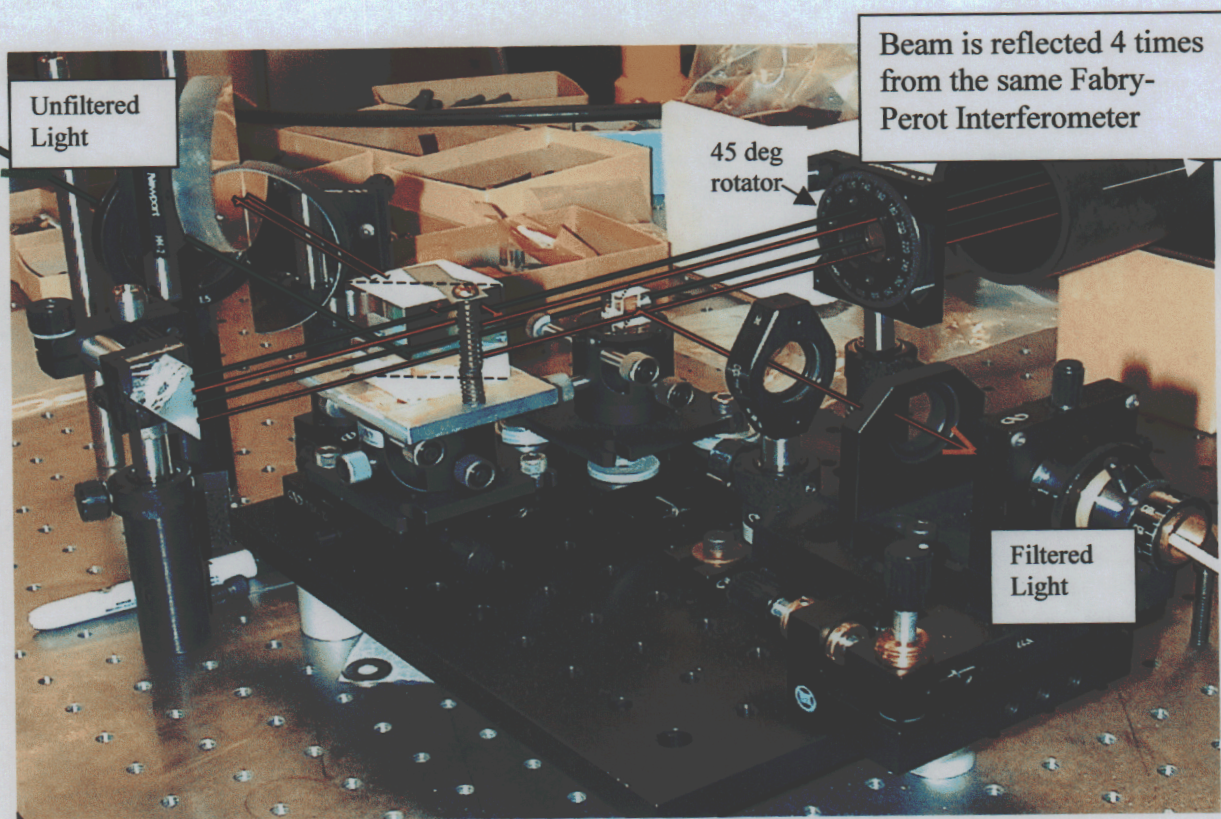

Figure 6. The high extinction ratio filter.

10. FUTURE PLANS

We are constructing another version of the filter, using both polarizations of the return light, in order to roughly double the efficiency, as shown in figure 7. With special fibers, one could in principle triple the efficiency. This scheme allows less margin for registration error between the lower two 7-fiber arrays.
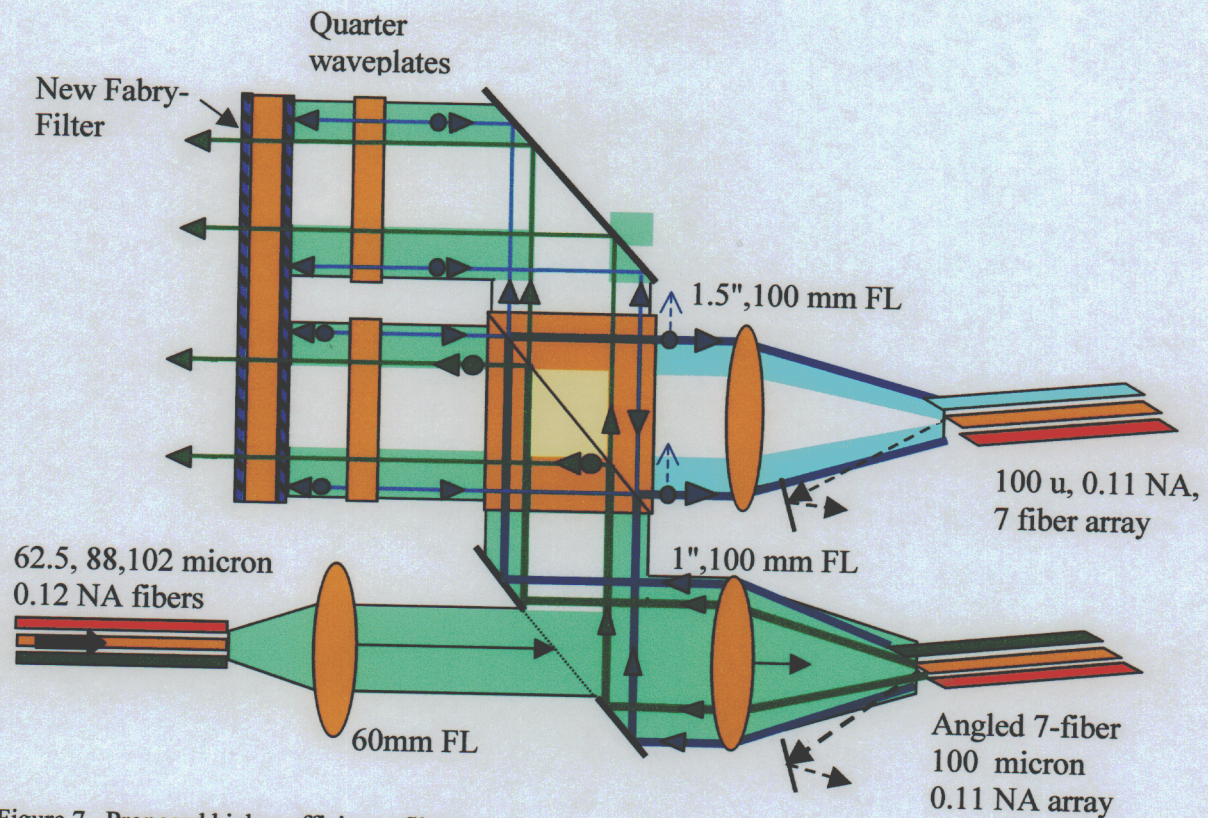
Figure 7. Proposed higher-efficiency filter

11. REFERENCES

1.   D. R. Goosman, "Formulas for Fabry-Perot velocimeter performance using both stripe and multifrequency techniques", Appl. Opt. **30** (27), 3907-3923 (1991).

2.   D. R. Goosman, G. Avara, L. Steinmetz, C. Lai and S. Perry, "Manybeam velocimeter for fast surfaces", SPIE proceedings on the 22nd Int. Congress on High Speed Photography and Photonics, **2869**, 1070-1079 (1996).

3.   Willard Hemsing, private communication

4.   C. Souers, private communication

5.   D. R. Goosman, A. M. Frank, H. H. Chau, and N. L. Parker, "Fabry-Perot Velocimetry Techniques: Is Doppler Shift Affected by Surface Normal Direction?", *Proc. High Speed Photography, Videography, and Photonics", Soc. Of Photo-Optical Instr. Engrs.* **427**, 127 (1983).

6.   J. M. Vaughan, "*The Fabry-Perot Interferometer*" (Adam Hilger,Bristol, 1989), Chap. 3.

7.   D. R. Goosman, George R. Avara and Stephen J. Perry, "Efficient optical probes for fast surface velocimetry: multiple frequency issues for Fabry and VISAR methods", SPIE proceedings on the 24th Int. Congress on High Speed Photography and Photonics, **4183**, 413-423 (2000).